

Hydrothermal Synthesis of Carbonate-Free Strontium Zirconate: Thermodynamic Modeling and Experimental Verification

Malgorzata M. Lencka,[‡] Erik Nielsen,[†] Andrzej Anderko,[‡] and Richard E. Riman^{*,†}

Department of Ceramics, College of Engineering, Rutgers, The State University of New Jersey, Piscataway, New Jersey 08855-0909, and OLI Systems, Inc., 108 American Road, Morris Plains, New Jersey 07950

Received August 21, 1996. Revised Manuscript Received February 26, 1997[®]

A comprehensive thermodynamic model has been applied to predict the optimum conditions for the hydrothermal synthesis of phase-pure strontium zirconate. The model is based on the accurate knowledge of standard-state thermochemical properties of all species and a realistic activity coefficient model. The predictions are conveniently summarized in the form of phase stability and yield diagrams. Unlike our previous works, the diagrams are automatically generated using newly developed software, which makes it possible to analyze the effect of reactant identity and concentrations, contaminants, pH, and temperature as independent variables. The calculations revealed a high sensitivity of the synthesis to the identity of Sr precursors, Sr/Zr molar ratio of starting materials, and temperature as well as to the contamination with carbonates. The predictions have been confirmed experimentally at two temperatures (433 and 473 K) using strontium hydroxide or strontium nitrate as sources of Sr and a hydrous zirconium dioxide as a source of Zr. Both the predictions and experiment demonstrate that phase-pure SrZrO₃ can be obtained only when all starting materials are CO₂-free.

Introduction

Recently, hydrothermal synthesis of perovskite-type ceramic materials has been extensively investigated using both theoretical and experimental techniques.^{1–6} It has been shown in our previous papers^{7–10} that accurate thermodynamic models can be constructed for a variety of hydrothermal systems of practical importance. These models make it possible to select effective, yet simple and inexpensive precursors and optimize process variables such as reagent concentrations, pH, temperature, and pressure. This methodology was applied to predict the optimum synthesis conditions for various perovskite-type^{7–10} materials. In all cases, the theoretical predictions were corroborated by experimental syntheses and efficient procedures were proposed for synthesizing phase-pure ceramic powders. In our previous studies,^{8–10} the thermodynamic predictions were summarized in the form of stability and yield diagrams

that show the conditions where ceramic powders are stable and can be obtained with a desired phase purity. The diagrams were constructed manually in a painstaking way by repetitive chemical and phase equilibrium computations for a wide range of reaction conditions. In the present study, we will present the results of computations obtained via computer software that automatically generates these diagrams. This software is integrated with OLI Systems' Environmental and Corrosion Simulation Programs.¹¹

Our computations will focus on conditions favoring the synthesis of strontium zirconate. In contrast to the abundant literature on the synthesis of compounds such as BaTiO₃ or PZT, relatively few researchers reported successful efforts to synthesize SrZrO₃ in hydrothermal media. Galkin and Chukhlantsev¹² outlined the synthesis of crystalline SrZrO₃ powder at temperatures from 473 to 623 K using Sr(OH)₂ and hydrous or anhydrous ZrO₂ with a Sr/Zr ratio ranging from 1.5 to 3. To avoid carbonate contamination, the Sr(OH)₂ was twice recrystallized and freed from carbonates and the synthesis was performed in CO₂-free atmosphere. The powders were washed with hot water, apparently to remove the excess of solid Sr(OH)₂, which is likely to form under these conditions. Kutty et al.¹³ also obtained pure SrZrO₃ at 663 K using Sr(OH)₂ and hydrothermally prepared ultrafine ZrO₂ (monoclinic) powder.

In this paper, we first apply our electrolyte solution model to compute the thermodynamic equilibrium states

[†] Rutgers.

[‡] OLI Systems, Inc.

[®] Abstract published in *Advance ACS Abstracts*, April 1, 1997.

(1) Dawson, W. *Ceram. Bull.* **1988**, *67*, 1673.

(2) Osseo-Asare, K.; Arriagada, F. J.; Adair, J. H. *Ceramic Transactions, Ceramic Powder Science IIA*; Messing, G. L., Fuller Jr., E. R., Hausner, H., Eds.; American Ceramic Society: Westerville, OH, 1988; Vol. 1, p 47.

(3) Kutty, T. R. N.; Vivekanandan, R. *Mater. Chem. Phys.* **1988**, *19*, 533.

(4) Klee, M. *J. Mater. Sci. Lett.* **1989**, *8*, 985.

(5) Kajiyoshi, K.; Ishizawa, N.; Yoshimura, M. *J. Am. Ceram. Soc.* **1991**, *74*, 369.

(6) Kutty, T. R. N.; Balachandran, R. *Mater. Res. Bull.* **1984**, *19*, 1479.

(7) Lencka, M. M.; Riman, R. E. *Chem. Mater.* **1993**, *5*, 61.

(8) Lencka, M. M.; Riman, R. E. *J. Am. Ceram. Soc.* **1993**, *76*, 2649.

(9) Lencka, M. M.; Anderko, A.; Riman, R. E. *J. Am. Ceram. Soc.* **1995**, *78*, 2609.

(10) Lencka, M. M.; Riman, R. E. *Chem. Mater.* **1995**, *7*, 18.

(11) Environmental and Corrosion Simulation Programs (ESP/CSP), OLI Systems, Inc., Morris Plains, NJ, 1996.

(12) Galkin, Yu. M.; Chukhlantsev, V. G. *Russ. J. Inorg. Chem.* **1966**, *11*, 119.

(13) Kutty, T. R. N.; Vivekanandan, R.; Philip, S. *J. Mater. Chem. Phys.* **1990**, *25*, 3649.

Table 1. Standard-State Properties of Individual Species in the Sr–Zr–CO₂ Hydrothermal System

aqueous species	Zr ⁴⁺	ZrOH ³⁺	Zr(OH) ₂ ²⁺	Zr(OH) ₃ ⁺	Zr(OH) ₅ ⁻	Zr(OH) ₄
ΔG_f° (kJ·mol ⁻¹)	-557.60	-796.63	-1022.1	-1240.1	-1652.2	-1451.0
ΔH_f° (kJ·mol ⁻¹)	-628.98	-889.1	-1140.6	-1395.8	-1966.2	-1675.4
S° (J·mol ⁻¹ ·K ⁻¹)	-461.5	-299.6	-153.5	-45.95	-109.9	-42.94
C_p° (J·mol ⁻¹ ·K ⁻¹)	-12.97	185.8	75.72	389.9	619.5	382.8
$V^\circ \cdot 10^6$ (m ³ ·mol ⁻¹)	-54.3	-12.70	14.46	22.86	34.53	36.92
ref	15	15	15	15	15	15
aqueous species	Zr ₃ (OH) ₄ ⁺⁸	Zr ₃ (OH) ₅ ⁺⁷	Zr ₄ (OH) ₈ ⁺⁸			
ΔG_f° (kJ·mol ⁻¹)	-2625.0	-2837.6	-4093.7			
ΔH_f° (kJ·mol ⁻¹)	-2958.0	-3195.3	-4518.1			
S° (J·mol ⁻¹ ·K ⁻¹)	-850.9	-700.8	-745.4			
ref	16, 17	16, 17	16, 17			
aqueous species	ZrCl ³⁺	ZrCl ₂ ²⁺	ZrCl ₃ ⁺	ZrCl ₄		
ΔG_f° (kJ·mol ⁻¹)	-697.85	-831.14	-962.72	-1093.7		
ΔH_f° (kJ·mol ⁻¹)	-776.98	-935.49	-1108.1	-1296.8		
S° (J·mol ⁻¹ ·K ⁻¹)	-310.7	-218.5	-179.4	-196.3		
C_p° (J·mol ⁻¹ ·K ⁻¹)	491.5	964.0	1404.5	1812.9		
$V^\circ \cdot 10^6$ (m ³ ·mol ⁻¹)	-33.77	-10.89	14.60	43.0		
ref	15	15	15	15		
solid species ^a	SrZrO ₃	ZrO ₂	ZrCl ₄			
ΔG_f° (kJ·mol ⁻¹)	-1681.7	-1039.7	-889.27			
ΔH_f° (kJ·mol ⁻¹)	-1767.3	-1097.5	-979.81			
S° (J·mol ⁻¹ ·K ⁻¹)	115.10	50.359	181.418			
C_p° (J·mol ⁻¹ ·K ⁻¹)	103.39	56.053	119.77			
a (J·mol ⁻¹ ·K ⁻¹)	124.064	69.5477	124.965			
$b \cdot 10^3$ (J·mol ⁻¹ ·K ⁻²)	12.217	7.6230	14.145			
$c \cdot 10^{-5}$ (J·mol ⁻¹ ·K)	-2.16156	-14.00	-8.36582			
$V^\circ \cdot 10^6$ (m ³ ·mol ⁻¹)	41.55	21.15	83.14			
ref	14, 19	14, 18	14, 19			

^a Heat capacities are calculated from the relation $C_p^\circ = a + bT + cT^{-2}$.

in the Sr–Zr–H₂O system and its Zr–H₂O subsystem. Then, we use the results of the computations to construct stability and yield diagrams, which serve as tools to determine the optimum synthesis conditions of phase-pure SrZrO₃. The predictions are specifically designed to take into account the effect of contamination with CO₂. Finally, we use the predictions to define the range of conditions for obtaining phase-pure SrZrO₃. These conditions are further verified in a series of experiments.

Theoretical Predictions

The theoretical model for rigorous simulation of thermodynamic equilibrium in heterogeneous, solid–liquid hydrothermal systems has been described in detail in a previous paper.⁷ To apply the model to a particular system, it is necessary to enumerate all solid, aqueous, and vapor species that may be important in the system. For these species, it is further required to specify the standard-state thermochemical properties, i.e., the standard Gibbs energies $\Delta_f G^\circ$, enthalpies $\Delta_f H^\circ$ of formation, and entropies S° at a reference temperature (298.15 K) as well as partial molar volumes V° and heat capacities C_p° as functions of temperature.

The thermochemical data^{14–19} for the species in the Sr–Zr–CO₂–H₂O system that have not been presented earlier^{9, 20} are listed in Table 1. The model utilizes these data in conjunction with a comprehensive activity

coefficient model²¹ to calculate the equilibrium concentrations of all species in all phases.

Repetitive application of the model for different input concentrations of Sr and Zr precursors as well as pH-adjusting agents (mineralizers) makes it possible to construct stability and yield diagrams, that show the reaction conditions for which a given product is stable and can be synthesized with an assumed yield.^{8–10} In this work, computer software has been developed for the automatic generation of these diagrams.

As the y -axis variable of both stability and yield diagrams, the program uses the input concentrations of one or more starting materials. The ratios of the concentrations can be held constant at a predetermined value. For example, the input concentrations of Sr(OH)₂ and ZrO₂ can be varied along the y -axis with their ratio kept constant at 1.0. As the x -axis variable, the program can use either pH or the input concentration of a pH-adjusting agent. If pH is chosen as the x -axis variable, the program changes the pH by adding varying amounts of a selected acid (such as HNO₃ or HCl) and a base (such as KOH or NaOH). If the input concentration of a pH-adjusting agent is chosen as the x -axis variable, it is varied by the program on a linear or

(14) Barin, I., in collaboration with Sauert, F.; Schultze-Rhonhof, E.; Shu Sheng, W. *Thermochemical Data of Pure Substances*; VCH Publishers: New York, 1989, 1993.

(15) Shock, E., private communication.

(16) Baes, C. F., Jr.; Mesmer, R. E. *The Hydrolysis of Cations*; Wiley-Interscience: New York, 1976.

(17) Slobodov, A. A.; Krickii, A. V.; Zarembo, V. I.; Puchkov, L. V. *Zh. Prikl. Khim.* **1992**, *65*, 1031.

(18) Robie, R. A.; Hemingway, B. S.; Fisher, J. R. *Thermodynamic Properties of Minerals and Related Substances at 298.15 K and 1 Bar (10⁵ Pascals) Pressure and at Higher Temperatures*. U.S. Geological Survey Bulletin 1452; U.S. Government Printing Office: Washington, DC, 1979.

(19) McLune, W. F., Ed. *Powder Diffraction File: Inorganic Phases*, JCPDS International Centre for Diffraction Data 1989, Swarthmore, PA, 1989.

(20) Lencka, M. M.; Riman, R. E. *Ferroelectrics* **1994**, *151*, 159.

(21) Rafal, M.; Berthold, J. W.; Scrivner, N. C.; Grise, S. L. *Models for Thermodynamic and Phase Equilibria Calculations*; Sandler, S. I., Ed.; Marcel Dekker, Inc.: New York, 1994; p 601.

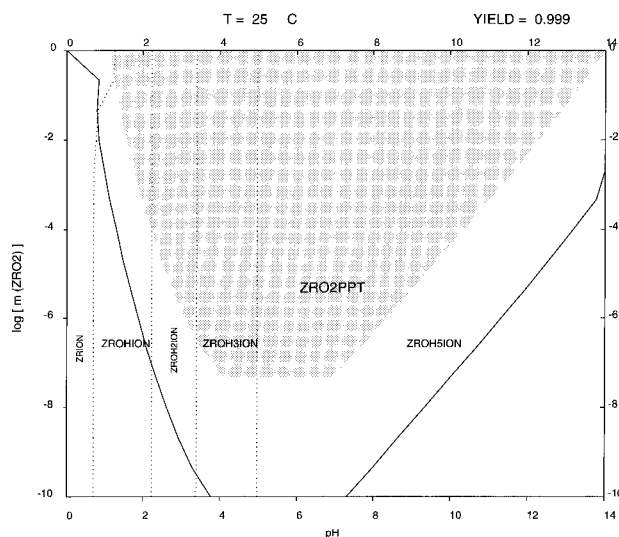


Figure 1. Calculated phase stability and yield diagram for the Zr hydrothermal system at 298 K. The symbols ZRO2PPT, ZRION, ZROHION, ZROH2ION, ZROH3ION, and ZROH5ION denote $\text{ZrO}_2(\text{s})$, Zr^{4+} , ZrOH^{3+} , $\text{Zr}(\text{OH})_2^{2+}$, $\text{Zr}(\text{OH})_3^+$, and $\text{Zr}(\text{OH})_5^-$, respectively.

logarithmic scale. It should be noted that the diagrams developed in previous papers^{7–10} were constructed always with pH as the x -axis variable. The automatic generation of diagrams allows us to be more flexible in the choice of independent variables. This is particularly useful when it is necessary to determine the amount of a pH-adjusting agent that is needed to obtain a certain yield of the product.

The stability diagrams include two types of lines: the solid lines denote the states of incipient precipitation of solids whereas the dotted lines show the loci where two aqueous species have equal concentrations. The yield diagrams show the areas where the desired product (e.g., SrZrO_3) precipitates with a yield greater than or equal to an assumed value (e.g., 99%). This yield is calculated by dividing the number of moles of the product by the total number of moles of the metal precursor. For example, the yield of SrZrO_3 can be calculated with respect to the total amount of Sr or Zr. The yield areas are shown in the diagrams as shaded fields.

Zr–H₂O System. First, it is worthwhile to investigate the phase behavior of the system Zr–H₂O in order to understand the properties of zirconium precursors, which are used for the synthesis of SrZrO_3 . Adair et al.^{22, 23} have previously calculated a stability diagram for ZrO_2 in water using the ideal solution approximation (i.e., with all activity coefficients set equal to one). In our work, however, we utilize a realistic model for solution nonideality.²¹ Figures 1 and 2 show combined stability and yield diagrams for the Zr–H₂O system at 298 and 433 K, respectively, as a function of pH of the solution and input molalities of zirconium species (m_{ZrO_2}). At low concentrations of Zr, the vertical lines separate the stability fields of Zr^{4+} , ZrOH^{3+} , $\text{Zr}(\text{OH})_2^{2+}$, $\text{Zr}(\text{OH})_3^+$, and $\text{Zr}(\text{OH})_5^-$. Although polynuclear zirco-

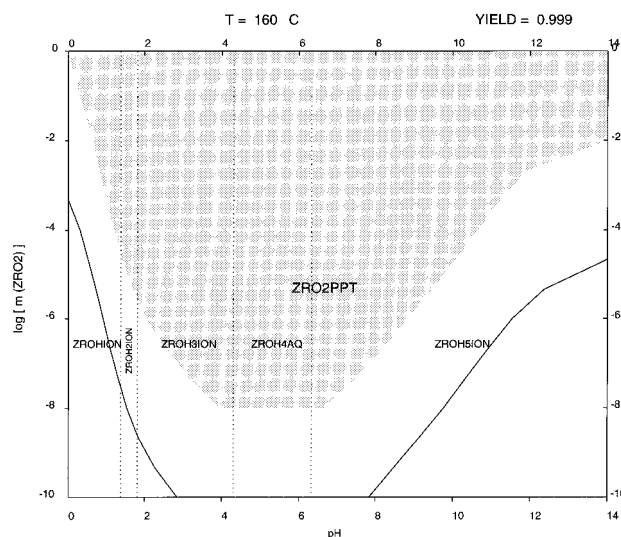


Figure 2. Calculated phase stability diagram for the Zr hydrothermal system at 433 K. The symbols ZRO2PPT, ZROHION, ZROH2ION, ZROH3ION, ZROH4AQ, and ZROH5ION denote $\text{ZrO}_2(\text{s})$, ZrOH^{3+} , $\text{Zr}(\text{OH})_2^{2+}$, $\text{Zr}(\text{OH})_3^+$, $\text{Zr}(\text{OH})_4(\text{aq})$, and $\text{Zr}(\text{OH})_5^-$, respectively.

nium species are present in the system (cf. Table 1), they are always much less abundant than the species shown in Figures 1 and 2. The incipient precipitation line for ZrO_2 has a parabolic shape and shows a minimum at about pH 5.5. In the acidic (low pH) region of the diagram, the incipient precipitation line slightly depends on the chemical identity of the acid that is used to adjust the solution pH. The solid line in Figure 1 was obtained with nitric acid. If HCl was used instead of HNO_3 , the incipient precipitation line in strongly acidic solutions would be somewhat shifted toward higher pH because HCl more easily solubilizes zirconia in the form of chloride complexes such as ZrCl_3^+ and ZrCl_2^{2+} .

The shaded areas show the loci where ZrO_2 will precipitate from the solution with a yield of more than 99.9%. It is worth noting that the region of 99.9% yield of ZrO_2 is very large and covers a wide pH range (e.g., from pH = 1.0 to pH = 14 at $m_{\text{ZrO}_2} = 1.0$). However, ZrO_2 can be solubilized in both very acidic and very alkaline environments. The stability of solid ZrO_2 is relatively weakly affected by temperature. As shown in Figure 2, the stability of ZrO_2 in a very acidic solution is somewhat higher at 433 K than at 298 K. For alkaline solutions, the temperature effect is very small. In such solutions, ZrO_2 dissolves and $\text{Zr}(\text{OH})_5^-$ becomes the dominant species for both temperatures. Our predictions are qualitatively similar to those obtained from an ideal-solution stability diagram.^{22, 23} Significant differences (by about 1 pH unit) are noted only for more concentrated solutions (i.e., above 0.01 M), especially in the strongly acidic and alkaline range.

Sr–Zr–H₂O System. For the calculation of the stability and yield diagrams for SrZrO_3 , we used ZrO_2 (monoclinic) as a source of Zr and strontium nitrate or hydroxide as source of Sr. Figures 3 and 4 show the calculated stability and yield diagrams for the Sr–Zr hydrothermal system at 433 and 473 K, respectively. The input concentrations of $\text{Sr}(\text{NO}_3)_2$ and ZrO_2 are used as independent variables with their ratio fixed at 1.0. In the homogeneous aqueous region, the dominant Sr species are Sr^{2+} , SrOH^+ , $\text{Sr}(\text{NO}_3)_2(\text{aq})$ and SrNO_3^+ . The

(22) Adair, J. H.; Denkwicz, R. P.; Arriagada, F. J.; Osseo-Asare, K. *Ceramic Transactions, Ceramic Powder Science IIA*; Messing, G. L., Fuller, E. R., Jr., Hausner, H., Eds.; American Ceramic Society: Westerville, OH, 1988; Vol. 1, p 135.

(23) Denkwicz, R. P., Jr.; TenHuisen, K. S.; Adair, J. H. *J. Mater. Res.* **1990**, *5*, 2698.

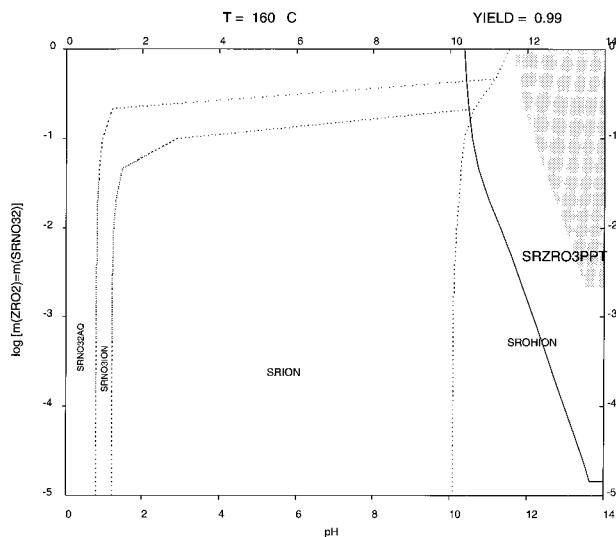


Figure 3. Calculated phase stability and yield diagram for the Sr–Zr hydrothermal system at 433 K for Sr/Zr = 1.0 using $\text{Sr}(\text{NO}_3)_2$ as a source of strontium. The symbols SRNO32AQ, SRNO3ION, SRION, SROHION, and SRZRO3PPT denote $\text{Sr}(\text{NO}_3)_2(\text{aq})$, SrNO_3^{3+} , Sr^{2+} , and SrOH^+ , respectively.

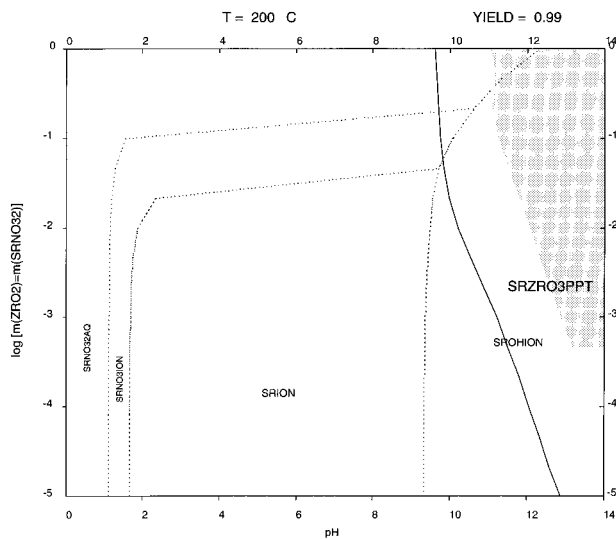


Figure 4. Calculated phase stability and yield diagram for the Sr–Zr hydrothermal system at 473 K for Sr/Zr = 1.0 using $\text{Sr}(\text{NO}_3)_2$ as a source of strontium.

nitrate complexes result from the presence of NO_3^- ions in $\text{Sr}(\text{NO}_3)_2$ as well as from the addition of nitric acid to vary pH. The stability of the $\text{Sr}(\text{NO}_3)_2(\text{aq})$ and SrNO_3^+ complexes in the aqueous phase may somewhat affect the yield diagram because it favors the presence of Sr species in solution and not in the solid phase. The precipitation of SrZrO_3 begins at pH values starting from 10.4 at 433 K and from 9.6 at 473 K when the input concentration of precursors is 1 *m*. These values increase as the solution becomes more dilute with respect to Sr and Zr. An increase of temperature by 40 K shifts the line downward by about 0.8–1 pH units depending on molality.

Figures 3 and 4 also show the calculated yield of SrZrO_3 as a function of pH and input molality of starting materials at 433 and 473 K, respectively. The region of nearly complete yield (above 99%) of strontium zirconate is very small and is much smaller than the stability region. The size of the complete yield region is somewhat influenced by the chemical identity of the

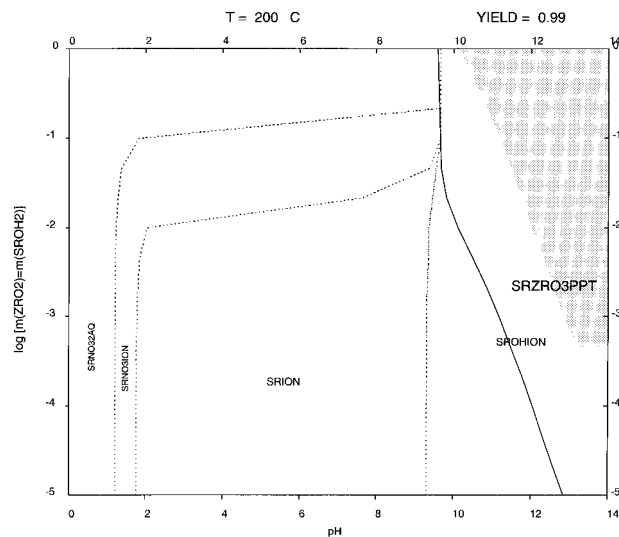


Figure 5. Calculated phase stability and yield diagram for the Sr–Zr hydrothermal system at 473 K for Sr/Zr = 1 using $\text{Sr}(\text{OH})_2$ as a source of strontium.

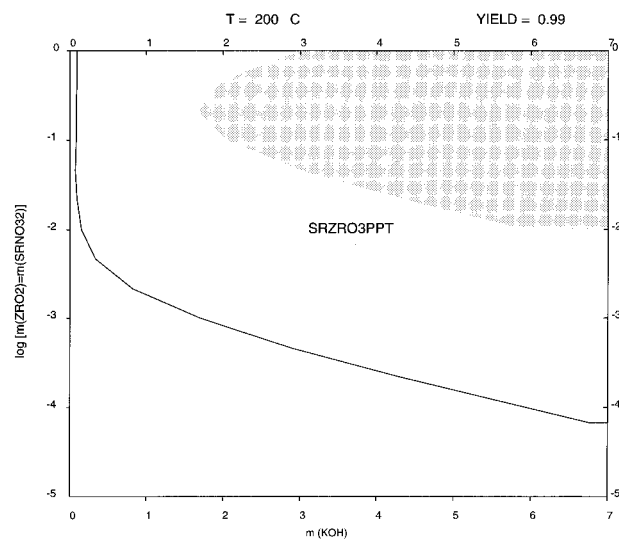


Figure 6. Calculated phase stability and yield diagram as a function of the input amount of KOH at 473 K for Sr/Zr = 1 using $\text{Sr}(\text{NO}_3)_2$ as a source of strontium.

Sr precursor and temperature. This is illustrated in Figure 5, which shows the stability and yield diagram at 473 K when $\text{Sr}(\text{NO}_3)_2$ is replaced by $\text{Sr}(\text{OH})_2$ as a source of Sr. The Sr precursor effects can be explained by specific interactions between ions in the solution, which affect the activity coefficients. In particular, we are dealing with the preferential formation of SrNO_3^+ and $\text{Sr}(\text{NO}_3)_2(\text{aq})$ at high molalities ($m_{\text{Sr}(\text{NO}_3)_2} > 0.1$), which shifts the equilibrium toward dissolved aqueous Sr species and away from the precipitation of SrZrO_3 . The nearly complete yield field somewhat widens with temperature (cf. Figures 3 and 4) in analogy to the stability field.

The stability and yield diagrams with pH as an independent variable (i.e., Figures 3–5) do not indicate how much of a pH-adjusting agent is necessary to synthesize the desired product. Therefore, we construct diagrams in which the Sr and Zr precursors, with a fixed molar ratio, are retained as *y*-axis variables and pH is replaced with the molality of a base (e.g., KOH) as an *x*-axis variable. Figures 6 and 7 show such diagrams at 473 K when $\text{Sr}(\text{NO}_3)_2$ and $\text{Sr}(\text{OH})_2$ are used as Sr

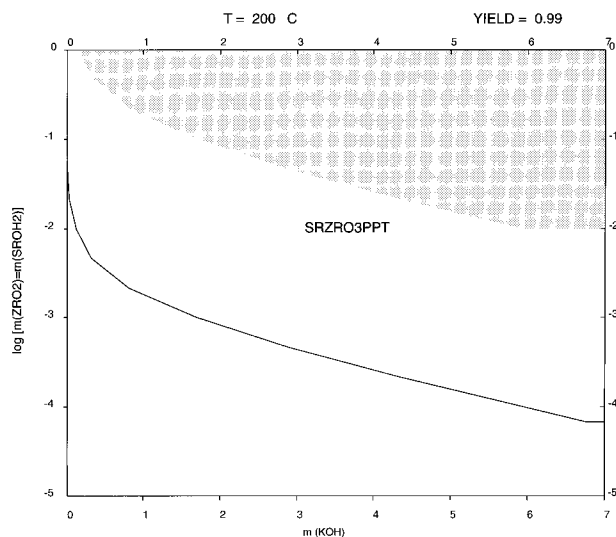


Figure 7. Calculated phase stability and yield diagram as a function of the input amount of KOH at 473 K for Sr/Zr = 1 using Sr(OH)₂ as a source of strontium.

sources, respectively. Figure 6 shows that a substantial molality of KOH is always necessary to precipitate phase-pure SrZrO₃ ($m_{\text{KOH}} > 1.6$). The necessary amount of KOH reaches a minimum when the amount of both Sr(NO₃)₂ and ZrO₂ is 0.22 *m*. It increases for both lower and higher input concentrations of starting materials. For practical purposes, an amount of KOH greater than 3 *m* is recommended. At lower temperatures, such as 433 K, the necessary amount of KOH increases to 4.5 *m* with a reduction in the area of the 99% yield region. If Sr(OH)₂ is used, the amount of KOH becomes much smaller but cannot be completely eliminated (see Figure 7). In this case, the minimum amount of KOH is as low as 0.2 *m* when the input concentration of Sr(OH)₂ is 1 *m* but rises to 1.6 *m* for an input concentration of 0.1 *m*.

Since the nearly complete yield region of SrZrO₃ is relatively small and limited to high pH and input molalities of Sr(NO₃)₂ and Sr(OH)₂, it was of interest to examine the influence of an excess amount of Sr precursor on the stability and yield. The excess amount of Sr may be introduced using Sr(NO₃)₂ or Sr(OH)₂ as starting materials. First, we consider Sr(NO₃)₂. Figure 8 shows the calculated yield diagram of SrZrO₃ at 473 K for the Sr/Zr ratio equal to 1.1. In this case, SrZrO₃ will be the first solid phase to precipitate from the solution as shown by the longer solid line in Figure 8. Within the nearly complete yield region of SrZrO₃ (shaded area), the excess amount of Sr precipitates as Sr(OH)₂. The precipitation of Sr(OH)₂ starts at the solid line that intersects the shaded area in Figure 8. At still higher pH values, more than 99% of the excess amount of Sr will precipitate as Sr(OH)₂. This is due to the fact that the solubility of Sr(OH)₂ is sufficiently low²⁴ for the nearly complete precipitation of the excess amount of Sr in very strongly alkaline solutions.

It is worthwhile to note that the excess of Sr in the solution shifts the equilibrium so that pure SrZrO₃ precipitates at lower pH values (cf. Figure 8, Sr/Zr = 1.1) and reduces the amount of the mineralizer. This

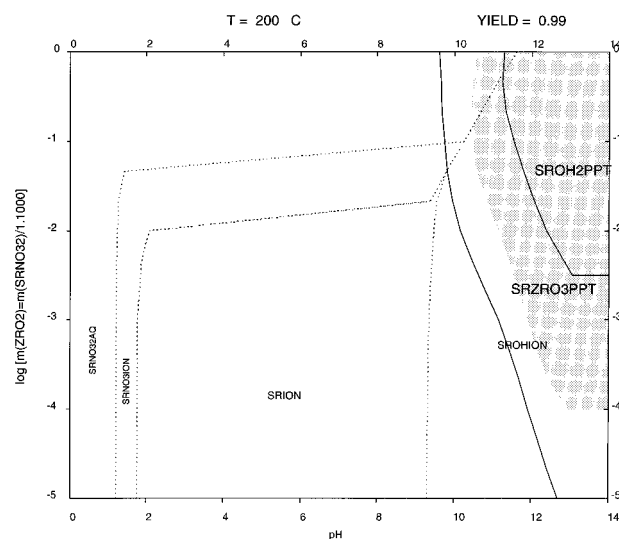


Figure 8. Calculated phase stability and yield diagram at 473 K for Sr/Zr = 1.1 using Sr(NO₃)₂ as a source of strontium.

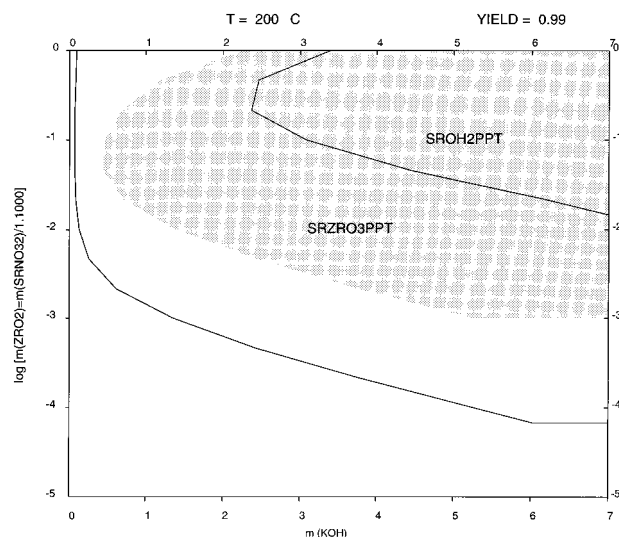


Figure 9. Calculated phase stability and yield diagram as a function of the input amount of KOH at 473 K for Sr/Zr = 1.1 using Sr(NO₃)₂ as a source of strontium.

is illustrated in Figure 9 on a plot versus the molality of KOH. Comparison of Figures 6 and 9 reveals that the nearly complete yield region is significantly enlarged by the excess amount of Sr. Consequently, a smaller amount of KOH is needed for the synthesis (i.e., 0.50 *m* solution of KOH as opposed to 2.05 *m* for $m_{\text{ZrO}_2} = 0.1$). Figure 10 illustrates what happens if we further increase the Sr/Zr ratio to 2.0. In this case, the minimum amount of KOH decreases to ca. 0.3 *m*, and the nearly complete yield region expands toward more dilute solutions. A similar trend is observed at $T = 433$ K. The only difference is a greater amount of mineralizer. For all Sr/Zr ratios greater than 1.0, the pH interval in which we can obtain pure SrZrO₃ (not contaminated by Sr(OH)₂) is limited and has a similar shape which is illustrated in Figures 9 and 10. In other words, an excess of Sr shifts both the 99% yield region and the beginning of precipitation of Sr(OH)₂ toward lower pH values. Thus, an excess of Sr is useful provided that the synthesis is performed in the pH region where Sr(OH)₂ does not precipitate. This point is illustrated in detail in Table 2, which shows the minimum and maximum amounts of KOH, for which phase-pure

(24) Linke, W. F.; Seidell, A. *Solubilities of Inorganic and Metal-Organic Compounds*, 4th ed.; American Chemical Society: Washington, D.C., 1965; Vol. 2, p 1514.

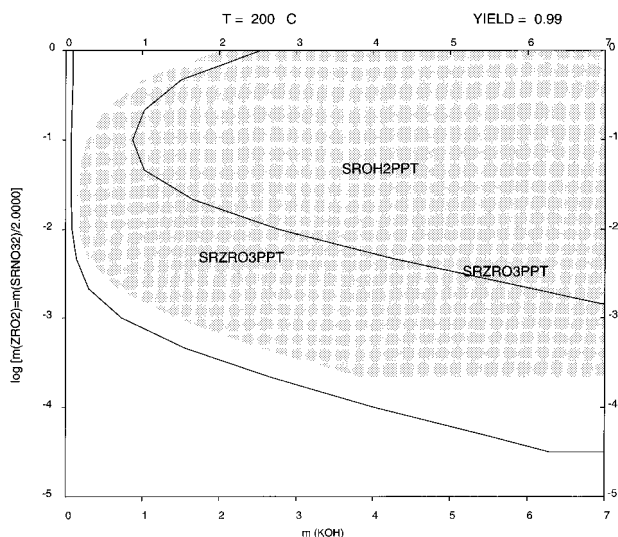


Figure 10. Calculated phase stability and yield diagram as a function of the input amount of KOH at 473 K for Sr/Zr = 2.0 using $\text{Sr}(\text{NO}_3)_2$ as a source of strontium.

SrZrO_3 is obtained with 99% yield without the precipitation of $\text{Sr}(\text{OH})_2$. As shown in Table 2, this “window” of KOH amounts strongly depends on the Sr/Zr precursor ratio and shifts to lower KOH amounts as the Sr/Zr ratio increases. The window becomes quite narrow when the initial concentration of starting materials is high (e.g., $m_{\text{ZrO}_2} = 1.0$).

Figure 11 shows the yield diagram for the Sr–Zr hydrothermal system at 473 K using $\text{Sr}(\text{OH})_2$ as a starting material. The Sr/Zr ratio is equal to 2.0. The beginning of precipitation of SrZrO_3 remains almost the same as in the case of $\text{Sr}(\text{NO}_3)_2$ (cf. Figure 10). The region of nearly complete yield of SrZrO_3 is much greater than for Sr/Zr = 1.0 and starts at lower amounts of KOH (cf. Figure 7) and correspondingly lower pH values (cf. Figure 5). Therefore, no mineralizer is necessary when the input concentration of Zr exceeds 0.02 m . The nearly complete yield fields in Figures 10 and 11 are similar except for the concentrated solutions ($m_{\text{ZrO}_2} > 0.01$) where the formation of complexes between Sr^{2+} and NO_3^- causes a difference.

As evident from the diagrams, an excess of Sr is very useful because it makes it possible to reduce the use of the mineralizer (for $\text{Sr}(\text{NO}_3)_2$ and $\text{Sr}(\text{OH})_2$) or eliminate it altogether (for $\text{Sr}(\text{OH})_2$). Subsequently, the probability of inclusion of extraneous cations (i.e., K^+) into the crystal lattice is reduced. For our working conditions ($m_{\text{ZrO}_2} = 0.1$), it is possible to calculate the range of Sr/Zr molar ratio for which no mineralizer is necessary and no $\text{Sr}(\text{OH})_2$ precipitates. Our calculations show that at 433 K this should be between 1.8 and 4.4, and for 473 K it should be between 1.2 and 2.6.

Effect of CO_2 Contamination. As described in the previous section, the synthesis of phase-pure SrZrO_3 is thermodynamically feasible when ZrO_2 is used with (1) $\text{Sr}(\text{NO}_3)_2$ and KOH for Sr/Zr ≥ 1.0 , where the amount of KOH is in the intervals shown in Table 2; (2) $\text{Sr}(\text{OH})_2$ for $1.8 < \text{Sr/Zr} < 4.4$ at 433 K and $1.2 < \text{Sr/Zr} < 2.6$ at 473 K for $m_{\text{ZrO}_2} = 0.1$ and without KOH.

There are many ways to introduce CO_2 into the Sr–Zr– H_2O system. Here, we classify them and assess their importance. We may introduce CO_2 (1) with starting materials (i.e., with $\text{Sr}(\text{OH})_2$, KOH, and hy-

drous ZrO_2); (2) during the preparation of the precursor solution by the absorption of CO_2 from air; (3) after the synthesis (i.e., during washing, filtration, etc.).

To eliminate the risk of carbonate contamination with starting materials, all reagents should be free from carbonates. However, carbonate-free $\text{Sr}(\text{OH})_2$, $\text{Sr}(\text{OH})_2 \cdot 8\text{H}_2\text{O}$, and KOH are not available commercially. Commercially available alkaline-earth hydrates usually contain 0.5–3 wt % of CO_2 . If all carbonate from this precursor was incorporated into the SrZrO_3 product, it may lead to a CO_2 content of 0.60–3.4 wt % in SrZrO_3 . The 99.99% (adjusted to cation) electronic grade KOH contains 0.4 wt % of K_2CO_3 according to the manufacturer (Aldrich). Assuming that all K_2CO_3 contained in KOH converts to SrCO_3 , the weight percent of SrCO_3 in the final product can be calculated. We can expect that using the Sr/Zr ratio greater than 1.0 would reduce the amount of SrCO_3 in our product. Our calculations show that for the Sr/Zr ratio equal to 1.0 and 2.0, SrZrO_3 will contain 2.1 and 0.32 wt % of SrCO_3 , respectively. At the same time, we can expect that the hydrolysis of zirconium isopropoxide which is used as a precursor in the presence of atmospheric CO_2 is accompanied by the formation of nonstoichiometric amorphous basic zirconium carbonate.^{25,26} This phenomenon takes place at pH values between 3.9 and 8.5–9.0.²⁵ It is reasonable to assume that the formation of hydrous ZrO_2 takes place within this pH range in our study.

The problem of contamination of the solution with carbonates during preparation of starting materials has been discussed in our previous paper.¹⁰ It was shown that the contact of alkaline strontium precursors with an open CO_2 -containing air atmosphere will lead to a contamination with SrCO_3 when the input concentration of Sr is greater than about $10^{-4} m$. Thus, it is beneficial to avoid the contact with atmosphere during the preparation of reagents and after the synthesis. However, the absorption of atmospheric CO_2 may require a substantial amount of time which could be much longer than the time required for experimental manipulations. Washing and vacuum filtering of the synthesis products in air may cause additional contamination, especially when an excess amount of strontium is present in alkaline environments. However, the existing carbonate content of starting materials appears to be the major determinant of the purity of the product. The relative importance of the sources of contamination of SrZrO_3 with SrCO_3 will be further identified in this study.

For further simulations, we assume that the CO_2 contamination results primarily from the CO_2 content of starting materials. Therefore, we have constructed stability diagrams in which the amount of CO_2 is varied proportionally to the amount of the Sr and Zr precursors. This simulates a real-world situation in which CO_2 is a fixed fraction of a reactant. Figure 12 shows the effect of CO_2 on the stability and yield diagram plotted against the pH when the input amount of CO_2 is equal to 0.085 times the amount of ZrO_2 . This amount corresponds to the average content of carbon dioxide in hydrous ZrO_2 and KOH in our reactions. Despite the small CO_2 content of the system, SrCO_3 is

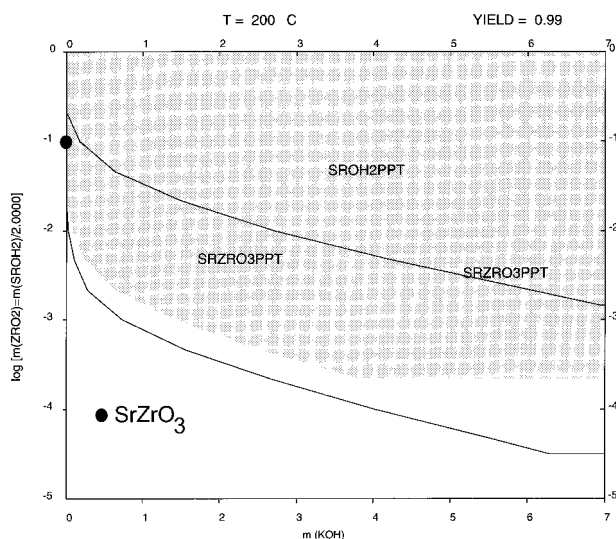
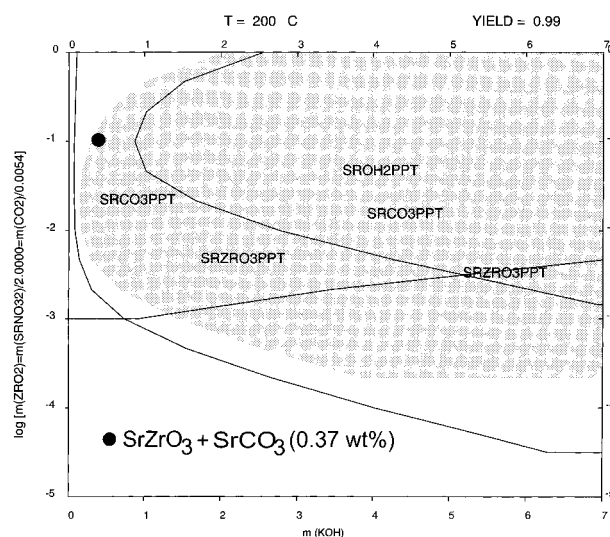
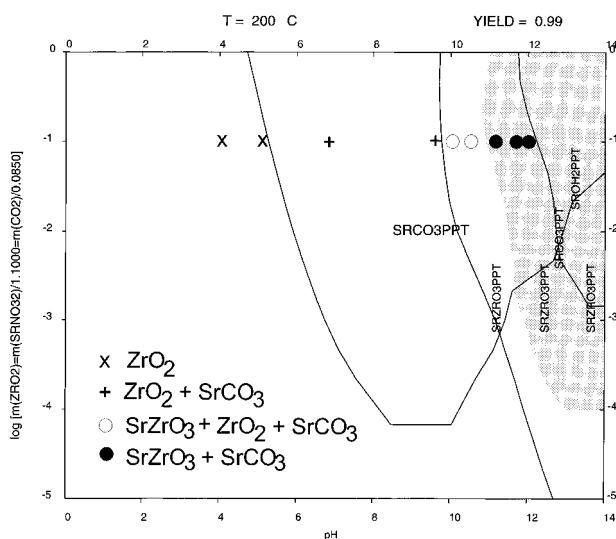
(25) Mikhailov, V. A.; Grigoreva, E. F. *Russ. J. Inorg. Chem.* **1961**, *6*, 760.

(26) Blumenthal, W. *Ind. Eng. Chem.* **1954**, *46*, 528.

Table 2. Ranges of KOH Amounts That Are Necessary To Obtain Phase-Pure SrZrO₃

$m_{\text{ZrO}_2} = 0.1$	$T = 433 \text{ K}$					$T = 473 \text{ K}$				
	1.0	1.05	1.1	2.0	5.0	1.0	1.05	1.1	2.0	5.0
Sr/Zr	1.0	1.05	1.1	2.0	5.0	1.0	1.05	1.1	2.0	5.0
m_{KOH} (min)	4.70	1.86	1.27	0.484	0.438	2.05	0.660	0.500	0.306	0.292
m_{KOH} (max)		7.71	5.90	1.89	1.40		4.68	3.28	0.920	0.750

$m_{\text{ZrO}_2} = 1.0$	$T = 433 \text{ K}$					$T = 473 \text{ K}$				
	1.0	1.05	1.1	2.0	5.0	1.0	1.05	1.1	2.0	5.0
Sr/Zr	1.0	1.05	1.1	2.0	5.0	1.0	1.05	1.1	2.0	5.0
m_{KOH} (min)	3.70	2.74	2.57	2.25	2.20	2.98	2.43	2.32	2.12	2.09
m_{KOH} (max)		4.89	4.16	2.99	2.85		3.95	3.47	2.64	2.49

**Figure 11.** Calculated phase stability and yield diagram as a function of the input amount of KOH at 473 K for Sr/Zr = 2.0 using Sr(OH)₂ as a source of strontium. The solid circle denotes experimental conditions for which phase-pure SrZrO₃ was obtained.**Figure 13.** Calculated phase stability and yield diagram at 473 K for Sr/Zr = 2.0 using Sr(NO₃)₂ as a source of strontium when the amount of CO₂ in the starting materials (i.e., KOH) is equal to 0.0054 times the amount of ZrO₂. The solid circle denotes experimental conditions for which SrZrO₃ contaminated with 0.37 wt % of SrCO₃ was obtained.**Figure 12.** Calculated phase stability and yield diagram at 473 K for Sr/Zr = 1.1 using Sr(NO₃)₂ as a source of strontium when the amount of CO₂ in the starting materials is equal to 0.085 times the amount of ZrO₂. The symbols denote experimental conditions for which the following products were obtained: (x) ZrO₂, (+) SrCO₃ + ZrO₂, (o) SrZrO₃ + ZrO₂ + SrCO₃, (●) SrZrO₃ + SrCO₃.

very stable and its stability range almost overlaps with the nearly complete yield range of SrZrO₃. SrZrO₃ is predicted to be carbonate-free only in dilute solutions at high pH values. Figure 13 shows an analogous diagram calculated with the input molality of KOH as an independent variable. In this case, the input amount

of CO₂ is approximately 16 times lower than that in Figure 12. Despite the lower CO₂ content, SrCO₃ remains stable and contaminates the product. The incipient precipitation line of SrCO₃ runs from the input molality of ZrO₂ equal to 0.001–0.005 *m* depending on the KOH input. Above this line, practically all CO₂ converts into SrCO₃ and precipitates. Thus, SrZrO₃ would be also contaminated with SrCO₃. For all practical purposes, CO₂ will always quantitatively precipitate in the 99% yield region of SrZrO₃ and contaminate the product even when the amount of CO₂ is very low. The carbonate contamination is practically independent of temperature. Moreover, the SrCO₃ does not significantly influence the stability and yield of SrZrO₃. Very similar behavior is observed when Sr(OH)₂ is used as source of Sr. This is illustrated in Figure 14 at *T* = 473 K.

Experimental Approach

To verify the theoretical predictions, experimental syntheses were performed using Sr(NO₃)₂ or Sr(OH)₂·8H₂O as sources of Sr and hydrous ZrO₂ as a source of Zr. The initial concentration of 0.1 *m* was chosen for ZrO₂ and KOH was used as a pH-adjusting agent. The Sr/Zr ratios ranging from 1.0 to 3.0 were used. Syntheses were performed at 433 and 473 K in the three regions of the stability and yield diagrams that were determined from the calculations, i.e., (1) Region of complete instability of SrZrO₃ (zero yield, outside the stability field of SrZrO₃). (2) Region of incomplete reaction (between the incipient precipitation line and nearly complete yield area). In both regions (1) and (2), reactions were performed for Sr/

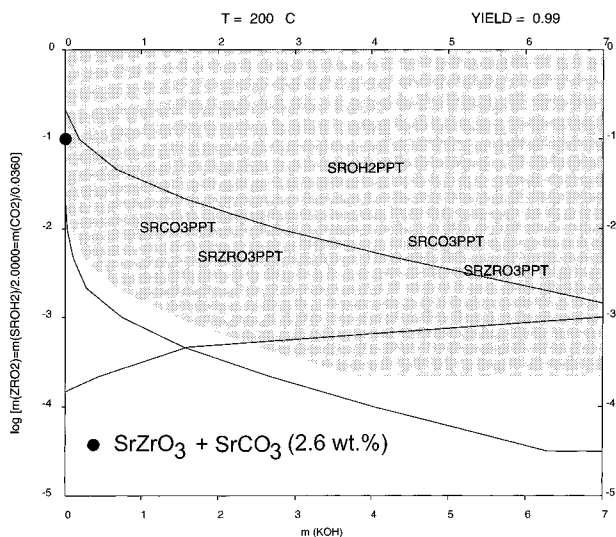


Figure 14. Calculated phase stability and yield diagram at 473 K for Sr/Zr = 2.0 using Sr(OH)₂ as a source of Sr when the amount of CO₂ in the starting materials (i.e., hydrous ZrO₂) is equal to 0.036 times the amount of ZrO₂. The solid circle denotes experimental conditions for which SrZrO₃ contaminated with 2.6 wt % of SrCO₃ was obtained.

Zr ratio equal to 1.0 and 1.1. (3) Region of nearly complete yield for various Sr/Zr ratios.

To compare theoretical predictions of stability of various solid phases as functions of temperature, input molality of reagents, Sr/Zr ratio and pH with experimentally precipitated products, 45 reactions were performed. The most representative ones are shown in Table 3 and in Figures 11–14. To identify the main source of CO₂ contamination in the Sr–Zr–CO₂–H₂O system, we performed our reactions with commercial CO₂-containing reagents, but all manipulations were carried out in an inert atmosphere. Then, the same procedure was repeated in air. Our standard procedure involved washing and vacuum filtration in air. However, to check if washing and filtering caused precipitation of additional SrCO₃ when the reactions are performed with Sr/Zr > 1, the resulting mixtures were washed and vacuum filtered in inert atmosphere instead. Finally, to investigate the influence of precursor purity on product (SrZrO₃) purity, precursors were synthesized or purified under inert atmosphere.

Characterization. For characterization, X-ray diffraction (XRD), thermogravimetric analysis (TGA), and electron microscopy analysis (SEM) were used. A wet chemical method²⁷ was employed to estimate the amount of carbonates in starting materials and products. The accuracy of this method has been estimated at ±2% of the detected amount of carbonates when the sample contains approximately 0.2–0.3 g of CO₂. To corroborate the existence and amount of SrCO₃ in the products, high-temperature (up to 1523 K) TGA (Perkin-Elmer, Norwalk, CT) was performed in air using a platinum pan with a heating rate 15 K/min. The evolution of CO₂ was observed at temperatures above 1170 K. Surface area analyses of various ZrO₂ powders were performed using single-point BET method and N₂ as an adsorbant. The XRD analyses were performed on a Siemens D-500 diffractometer (Siemens Analytical X-ray Instruments Inc., Madison, WI). The products were identified by comparing the experimental X-ray patterns to standards compiled by the Joint Committee on Powder Diffraction and Standards¹⁹ (JCPDS). The morphology of the particles was examined using scanning electron microscopy (SEM, AMRAY 1400T, Bedford, MA). Selected area electron diffraction analysis was performed to determine the crystallinity of the obtained powders. Finally, Fourier transform infrared (FTIR) spectroscopy (Model 1720/X, Perkin-Elmer, Norwalk, CT) was

used to detect species derived from carbon dioxide exposure. Spectra were compiled from 70 scans measured between 4000 and 400 cm⁻¹ with 4 cm⁻¹ resolution.

Reagents and Procedures. As reagents, Sr(NO₃)₂ (Fisher Scientific, Fair Lawn, NJ, >99.9%), Sr(OH)₂·8H₂O (Johnson Matthey, Alfa Aesar, Ward Hill, MA, >99.9 wt % on metal basis) were used. In our previous paper,⁹ we found that crystalline ZrO₂ was not sufficiently reactive to react quantitatively with the aqueous cations. The hydrous zirconia is an amorphous, nanostructured, high-surface-area powder. Its reactivity is due to the large surface area. According to BET measurements, the specific area of hydrous ZrO₂ is 272 m²/g, whereas that of crystalline ZrO₂ is 4.9 and 18.3 m²/g for the commercial powders of Fisher and Tosoh (Shuo-ku, Tokyo, Japan), respectively. Therefore, we used freshly precipitated hydrous ZrO₂, as described in our previous paper.⁹ To adjust pH, KOH (Aldrich, Chemical Co., Milwaukee, WI, semiconductor grade, 99.99 wt % on metal basis) was used. For the reactions that were performed in an inert gas (Ar) atmosphere, a glovebox (VAC Vacuum Atmosphere Co., Model DLX-001-S-P, Hawthorne, CA) was used. The amount of CO₂ in freshly precipitated hydrous ZrO₂ was estimated using the wet chemical method²⁷ described earlier. Our ZrO₂ powders contain about 1.3 wt % of CO₂. The small content of CO₂ in hydrous ZrO₂ precludes its detection by TGA analysis which shows a smooth gradual weight loss of about 32–34 wt % to 700 K. Beyond 700 K, no further weight loss is observed. This loss is due to the evolution of water, organic residuals and CO₂. Also, we checked Sr(OH)₂·8H₂O for CO₂ content using the same wet chemical method. It was revealed that Sr(OH)₂·8H₂O contained approximately 1.0 wt % of CO₂. This prompted us to purify this reactant. For this purpose, we removed SrCO₃ by filtering SrCO₃ contaminants from a hot stock solution of Sr(OH)₂·8H₂O. The obtained stock solution has been used for the reactions within the region of nearly complete yield of SrZrO₃. Commercial KOH contained 0.4 wt % of K₂CO₃ according to our wet chemical analysis, which was in agreement with the manufacturer's specification. KOH was used as received.

The reagents were charged into 125-mL stainless steel Teflon-lined autoclaves (Parr Instrument Co., Moline, IL). They occupied about 70% of the volume. The pressure in the vessel was autogenous and can be estimated at 6 atm at 433 K and at 15 atm at 473 K. The experimental setup was designed to avoid temperature gradients within the vessel as described in a previous paper.¹⁰ The vessel was maintained at the experimental temperature (433 or 473 K) for 48–60 h to ensure the complete equilibration. No stirring was employed because it was found to have no influence on the reactions in our system.

Results and Discussion

1. Synthesis in the Region of Thermodynamic Instability of SrZrO₃. As expected, the reactions performed in the zero yield area using commercial Sr(OH)₂·8H₂O in conjunction with HNO₃ and CO₂-containing hydrous ZrO₂ (cf. reaction 1a from Table 3) gave only poorly crystallized ZrO₂ (monoclinic, JCPDS No. 37-1484 and tetragonal, JCPDS No. 24-1164), which is due to a transformation of amorphous hydrous ZrO₂. Even though both ZrO₂ and Sr(OH)₂·8H₂O contain CO₂, SrCO₃ does not precipitate because it is not stable at these low pH values. Reactions performed with Sr(NO₃)₂ and CO₂-containing hydrous ZrO₂ also resulted in a mixture of tetragonal and monoclinic ZrO₂ (cf. reaction 2a in Table 3). The same reaction was performed with a small amount of KOH (cf. Table 3, reaction 1) in a glovebox and precipitated a mixture of ZrO₂ and SrCO₃ (orthorhombic, JCPDS No. 5-418) where the primary source of carbonate was from amorphous ZrO₂, indicating that the zirconium precursor can act as a source of contamination of SrZrO₃ with carbonates. The above

(27) Elwell, W. T.; Wood, D. F. *Comprehensive Analytical Chemistry*; Wilson, C. L., Wilson, D. W., Eds.; Elsevier Publishing: New York, 1962; Vol. 1C, p 140.

Table 3. Synthesis Conditions and Results^a

no.	precursors	Sr/Zr ratio	T/K	<i>m</i> _{KOH}	pH	calcd stable phases	products detected by XRD	wt % of CO ₂		
								calcd	TGA	chem anal.
Initial Precursors Solution Prepared in Inert Gas Atmosphere										
1	Sr(NO ₃) ₂ ZrO ₂ , CO ₂ -containing	1.1	433	0.09	10.1	ZrO ₂ SrCO ₃	ZrO ₂ SrCO ₃	1.3	1.2	
2	Sr(NO ₃) ₂ ZrO ₂ , CO ₂ -containing	1.1	473	0.09	9.76	SrZrO ₃ ZrO ₂ SrCO ₃	SrZrO ₃ ZrO ₂ SrCO ₃	1.3	1.2	
3	Sr(OH) ₂ , CO ₂ -containing ZrO ₂ , CO ₂ -free	1.1	473	HNO ₃	9.65	SrZrO ₃ ZrO ₂ SrCO ₃	SrZrO ₃ ZrO ₂ SrCO ₃	2.1	2.2	
4	Sr(NO ₃) ₂ ZrO ₂ , CO ₂ -containing	1.1	473	3.5	11.7	SrZrO ₃ SrCO ₃	SrZrO ₃ SrCO ₃	1.9	1.7	2.0
5	Sr(NO ₃) ₂ ZrO ₂ , CO ₂ -containing	1.4	433	2.5	11.7	SrZrO ₃ SrCO ₃	SrZrO ₃ SrCO ₃	1.5	1.6	1.4
6	Sr(NO ₃) ₂ ZrO ₂ , CO ₂ -containing	1.4	473	0.8	10.7	SrZrO ₃ SrCO ₃	SrZrO ₃ SrCO ₃	1.0	1.1	1.0
7	Sr(NO ₃) ₂ ZrO ₂ , CO ₂ -containing	2.0	473	0.33	9.76	SrZrO ₃ SrCO ₃	SrZrO ₃ SrCO ₃	0.8	1.0	
8	Sr(NO ₃) ₂ ZrO ₂ , CO ₂ -free	1.1	473	3.3	11.5	SrZrO ₃ SrCO ₃	SrZrO ₃ SrCO ₃	1.0	0.8	0.6
9 ^a	Sr(NO ₃) ₂ ZrO ₂ , CO ₂ -free	1.1	473	3.3	11.5	SrZrO ₃ SrCO ₃	SrZrO ₃ SrCO ₃	1.0	0.6	0.5
10	Sr(NO ₃) ₂ ZrO ₂ , CO ₂ -free	2.0	473	0.33	9.78	SrZrO ₃ SrCO ₃	SrZrO ₃ SrCO ₃	0.1	0.2	0.1
11 ^b	Sr(NO ₃) ₂ ZrO ₂ , CO ₂ -free	2.0	473	0.33	9.78	SrZrO ₃ SrCO ₃	SrZrO ₃ SrCO ₃	0.1	0.2	0.1
12	Sr(OH) ₂ , CO ₂ -containing ZrO ₂ , CO ₂ -containing	1.7	473		9.91	SrZrO ₃ SrCO ₃	SrZrO ₃ SrCO ₃	2.6	3.7	
13	Sr(OH) ₂ , CO ₂ -containing ZrO ₂ , CO ₂ -containing	2.5	473		10.2	SrZrO ₃ SrCO ₃	SrZrO ₃ SrCO ₃	3.5	4.6	
14	Sr(OH) ₂ , CO ₂ -free ZrO ₂ , CO ₂ -free	1.5	473		9.90	SrZrO ₃	SrZrO ₃	0	0	
15	Sr(OH) ₂ , CO ₂ -free ZrO ₂ , CO ₂ -free	2.0	473		10.1	SrZrO ₃	SrZrO ₃	0	0	0
Initial Precursors Solution Prepared in Air										
1a	Sr(OH) ₂ , CO ₂ -containing ZrO ₂ , CO ₂ -containing	1.1	433	HNO ₃	4.50	ZrO ₂	ZrO ₂			
2a	Sr(NO ₃) ₂ ZrO ₂ , CO ₂ -containing	1.1	473		4.80	ZrO ₂	ZrO ₂			
3a	Sr(NO ₃) ₂ ZrO ₂ , CO ₂ -containing	1.4	433	2.5	11.7	SrZrO ₃ SrCO ₃	SrZrO ₃ SrCO ₃	1.5	1.6	1.3
4a	Sr(NO ₃) ₂ ZrO ₂ , CO ₂ -containing	1.4	473	0.8	10.7	SrZrO ₃ SrCO ₃	SrZrO ₃ SrCO ₃	1.0	1.2	0.9
5a	Sr(OH) ₂ , CO ₂ -containing ZrO ₂ , CO ₂ -containing	1.5	473		9.85	SrZrO ₃ SrCO ₃	SrZrO ₃ SrCO ₃	2.1	2.2	
6a	Sr(OH) ₂ , CO ₂ -free ZrO ₂ , CO ₂ -containing	2.0	433		10.5	SrZrO ₃ SrCO ₃	SrZrO ₃ SrCO ₃	0.70		0.60
7a	Sr(OH) ₂ , CO ₂ -free ZrO ₂ , CO ₂ -containing	3.0	433		10.7	SrZrO ₃ SrCO ₃	SrZrO ₃ SrCO ₃	0.70	0.8	0.70
8a	Sr(OH) ₂ , CO ₂ -free ZrO ₂ , CO ₂ -containing	1.5	473		9.88	SrZrO ₃ SrCO ₃	SrZrO ₃ SrCO ₃	0.70		0.80
9a	Sr(OH) ₂ , CO ₂ -free ZrO ₂ , CO ₂ -containing	2.0	473		10.1	SrZrO ₃ SrCO ₃	SrZrO ₃ SrCO ₃	0.70	0.7	0.90

^a Filtration and washing performed in inert gas.

results are in very good agreement with the predictions of our thermodynamic model which is illustrated in Figure 12 with symbols × and + and in Table 3 (reactions 1a, 2a and 1).

2. Synthesis in the Region of Thermodynamic Stability of SrZrO₃ but outside the Complete Yield Region. In the region of incomplete reaction, we have obtained a mixture of SrZrO₃ (orthorhombic, JCPDS No. 10-268), SrCO₃ and ZrO₂ (cf. reactions 2 and 3, Table 3). When Sr(NO₃)₂ was used in conjunction with a small amount of KOH (cf. reaction 2) or Sr(OH)₂·8H₂O was used with HNO₃ (cf. reaction 3), we obtained SrZrO₃ and ZrO₂ in varying proportions, depending on the pH, and SrCO₃. The detected amounts of SrCO₃ agree very well with the amounts predicted by our model assuming that all reagents (i.e., hydrous ZrO₂ and KOH or Sr(OH)₂·8H₂O) contain carbonates. Since all reactions from this

region were performed in inert gas atmosphere, it appears that carbonate contamination is mainly due to the CO₂ content of starting materials.

3. Synthesis in the Region of Thermodynamic Stability of SrZrO₃. As expected, reactions performed in the complete yield region of SrZrO₃ gave SrZrO₃ and SrCO₃ or phase-pure SrZrO₃ depending on the purity of precursors. SrZrO₃ and SrCO₃ were obtained from the reaction 4 (cf. Table 3) which was performed using all CO₂-containing reagents. The calculated content of CO₂ is 1.9 wt %. TGA analysis shows the decomposition of SrCO₃ at approximately 1173–1223 K which is lower than the decomposition of pure SrCO₃ (i.e., 1373 K²⁸). This may be caused by the small particle size of hydrothermal SrCO₃. The CO₂ content calculated from the weight loss and wet chemical analysis is 1.7 and 2.0 wt %, respectively. Similar reactions performed

with lower amounts of KOH and different Sr/Zr ratios also resulted in the formation of SrZrO₃ and SrCO₃ (cf. Table 3, reactions 5–7). Calculated amounts of CO₂ present in SrZrO₃ agree very well with those obtained from TGA and wet chemical analysis. It was of interest to repeat the same reactions in air in order to elucidate whether contact with air increases the amount of CO₂ in our product. Reactions 3a and 4a are representative for these experiments and can be compared to reactions 5 and 6. As shown in Table 3, no significant influence of air is observed. Reactions performed with CO₂-free ZrO₂, Sr(NO₃)₂, and various amounts of commercial KOH gave also SrZrO₃ contaminated with SrCO₃ (cf. Table 3, reactions 8 and 10). SrCO₃ was not detectable by XRD in some cases (e.g., reaction 10) because of its small content in SrZrO₃. The calculated amounts of CO₂ in SrZrO₃ are also in good agreement with those detected by TGA and wet chemical analysis. Products of analogous reactions (cf. reactions 9 and 11) washed and vacuum filtered in inert gas atmosphere show amounts of CO₂ that are similar to those in reaction 8 and 10. This confirms our conclusion that carbonate contamination of our product results from the carbonate contamination of precursors. Reactions 12 and 13 were performed using CO₂-containing Sr(OH)₂·8H₂O and ZrO₂ without any KOH. According to our calculations, SrZrO₃ formed with SrCO₃ contamination. Here, the experimental amount of CO₂ is somewhat greater than the calculated amount which is probably due to the variation of CO₂ content within the large Sr(OH)₂·8H₂O crystals. Similar reaction (cf. reaction 5a) performed in air did not introduce additional carbonate contamination. Reactions performed with CO₂-free Sr(OH)₂·8H₂O (cf. reactions 6a–9a) resulted in formation of SrZrO₃ and SrCO₃. In this case, contamination results from carbonate content of hydrous ZrO₂, and the agreement between experimental and calculated amounts of CO₂ is very good. This may signify that carbonate content of ZrO₂ is equally distributed within fine particles of ZrO₂ in contrast to the SrCO₃ content in Sr(OH)₂·8H₂O crystals. Finally, reactions performed with CO₂-free Sr(OH)₂·8H₂O and ZrO₂ gave phase-pure SrZrO₃ as confirmed by TGA and wet chemical analysis (cf. Table 3, reactions 14 and 15). FTIR spectra supported these findings by showing no evidence of carbonates as well. Thus, in this case, we can conclude that we have substantially reduced or eliminated carbonate species, whether they are amorphous or crystalline.

The results of our experiments show very good agreement with the predictions of our thermodynamic model. The model is fully validated because it correctly predicts the formation of all phases that are observed in the system and, at the same time, gives their amounts with high accuracy. Selected experimental conditions and produced phases (not necessarily included in Table 3) are also shown in Figures 11–14. The amount of CO₂ in Figure 12 corresponds to the average CO₂ content in

all reactions performed with Sr(NO₃)₂ at 473 K for Sr/Zr = 1.1. Small variations of carbon dioxide content do not affect the phase boundaries.

4. Physical Characteristics. Characteristic spotted selected area electron diffraction patterns indicated that the particles of SrZrO₃ are monocrystalline. The shape of the particles strongly depends on the chemical identity of starting materials. They have diverse shapes with dimensions ranging from 0.2 to 1.5 μm. In particular, cubelike particles are obtained when Sr(NO₃)₂ and KOH are used, rounded shapes are noted if NaOH was used instead of KOH, and clusters of crystallites are obtained from Sr(OH)₂·8H₂O.

Conclusions

Electrolyte thermodynamics, coupled with a facility for the automatic generation of stability and yield diagrams, provides a powerful tool for predicting the effect of various process conditions on the synthesis of SrZrO₃. The model is particularly valuable for analyzing the effects of changing the chemical identity and relative amounts of starting materials as well as for predicting the possibility of contamination with carbonates. The theoretical predictions allow us to formulate synthesis guidelines. These guidelines strongly depend on whether CO₂ is present or absent in the starting materials. If the reactants do not contain CO₂ and all manipulations are performed in CO₂-free atmosphere, it is better to use Sr(OH)₂ rather than Sr(NO₃)₂ with the Sr/Zr ratio varying from 1.2 to 4.4 at $T = 433$ K and from 1.8 to 2.7 at $T = 473$ K. The appropriate Sr/Zr ratio ensures that the precipitation of the excess amount of Sr in the form of Sr(OH)₂ is avoided. If a certain level of contamination with CO₂ cannot be avoided, it is necessary to maintain the Sr/Zr ratio above 1.0. Otherwise, unreacted ZrO₂ will remain in the product. It may be then advantageous to use Sr(NO₃)₂ in conjunction with KOH because Sr(NO₃)₂ is not likely to contain carbonates. If this is the case, the Sr/Zr ratio between 1.05 and 2.0 is then recommended because it minimizes the necessary amount of KOH. Also, larger amounts of KOH are not advisable because they may cause the precipitation of undesirable Sr(OH)₂. Irrespectively of whether CO₂ is present or not, it is advisable to perform the syntheses at higher temperatures (i.e., 473 as opposed to 433 K) because the 99 mol % yield region field is larger and smaller amounts of KOH are required.

Acknowledgment. We gratefully acknowledge the generous support of the Material Division (Code 1131) at the Office of Naval Research (ONR) under the auspices of the ONR Young Investigator Program. The work at OLI Systems was sponsored by ONR under Contract N00014-95-C-0260. The authors thank Ms. Lynda Renomeron and Ms. Madeline Roepcke for their assistance.

CM960444N

(28) Solvay Barium Strontium GmbH, *Strontium Carbonate*, Hannover, Germany.